Mon. Not. R. Astron. Soc. **000**, 000–000 (0000) Printed 21 June 2018 (MN LATEX style file v2.2)

Galaxy pairs in the Sloan Digital Sky Survey - VI. The orbital extent of enhanced star formation in interacting galaxies

David R. Patton[1], Paul Torrey[2], Sara L. Ellison[3], J. Trevor Mendel[3] and Jillian M. Scudder[3]
[1] *Department of Physics and Astronomy, Trent University, 1600 West Bank Drive, Peterborough, ON K9J 7B8, Canada.*
[2] *Harvard Smithsonian Center for Astrophysics, 60 Garden Street, Cambridge, MA 02138, USA*
[3] *Department of Physics and Astronomy, University of Victoria, Victoria, BC V8P 1A1, Canada*

21 June 2018

ABSTRACT

We use pair and environmental classifications of ∼ 211 000 star-forming galaxies from the Sloan Digital Sky Survey, along with a suite of merger simulations, to investigate the enhancement of star formation as a function of separation in galaxy pairs. Using a new technique for distinguishing between the influence of nearby neighbours and larger scale environment, we find a clear enhancement in star formation out to projected separations of ∼ 150 kpc, beyond which there is no net enhancement. We find the strongest enhancements at the smallest separations (especially < 20 kpc), consistent with earlier work. Similar trends are seen in the simulations, which indicate that the strongest enhancements are produced in highly disturbed systems approaching final coalescence, whereas the more modest enhancements seen at wider separations are the result of starburst activity triggered at first pericentre passage, which persists as the galaxies move to larger separations. The absence of any net enhancement beyond 150 kpc provides reassurance that the detected enhancements are due to galaxy−galaxy interactions, rather than larger scale environmental effects or potential pair selection biases. A rough census indicates that 66 per cent of the enhanced star formation in our pair sample occurs at separations > 30 kpc. We conclude that significant interaction-induced star formation is not restricted to merger remnants or galaxies with close companions; instead, a larger population of wider separation pairs exhibit enhanced star formation due to recent close encounters.

Key words: galaxies: evolution − galaxies: interactions − galaxies: star formation.

1 INTRODUCTION

The observational study of close galaxy pairs has revealed clear evidence of enhanced star formation rates (SFRs) in interacting and merging galaxies. The strongest enhancements are found in the closest pairs, with projected separations $\lesssim$ 30 kpc (e.g., Barton, Geller, & Kenyon 2000; Lambas et al. 2003; Ellison et al. 2008; Freedman Woods et al. 2010). These enhancements are consistent with interaction-induced star formation seen in simulations of merging galaxies, with the closest pairs comprised of systems seen near their first pericentre passage, as well as those which are coalescing (e.g., Mihos & Hernquist 1996; Di Matteo et al. 2007; Cox et al. 2008; Montuori et al. 2010).

More recently, Scudder et al. (2012) have shown that SFR enhancements are present out to the 80 kpc limit of their pairs sample. These enhancements are accompanied by bluer central colours (Patton et al. 2011), diluted metallicities (Scudder et al. 2012), and an increased incidence of active galactic nuclei (AGNs; Ellison et al. 2011) and luminous infrared galaxies (Ellison et al. 2013). While some studies have probed enhanced star formation out to even larger separations, it is unclear if these enhancements are due to galaxy−galaxy interactions, larger scale environmental effects or sample biases (e.g., Sol Alonso et al. 2006; Park et al. 2007; Robaina et al. 2009; Robaina & Bell 2012).

This leaves open a crucial question: at what projected separations do interaction-driven enhancements disappear? The answer to this question is needed for a full accounting of the contributions of interaction-induced star formation to the cosmic SFR, and can also provide insight into the orbits of interacting galaxies. The orbital extent of enhanced star formation depends on a number of factors, such as the energies and angular momenta of pair orbits, the strength and duration of induced star formation, the availability and distribution of gas, stellar and AGN feedback, the amount of contamination by non-interacting pairs (e.g., chance superpositions within groups or clusters), etc.

With this Letter, we address this question using a spectroscopic sample of Sloan Digital Sky Survey (SDSS)[1] galaxy pairs which extends out to much larger separations than earlier work, and which carefully controls for environment. We then compare

[1] sdss.org

our findings with predictions from a suite of merger simulations spanning a range of orbital eccentricities, impact parameters and disc orientations. We adopt a concordance cosmology of $\Omega_\Lambda = 0.7$, $\Omega_M = 0.3$ and $H_0 = 70\ h_{70}$ km s^{-1}Mpc^{-1} throughout.

2 SAMPLE SELECTION

2.1 Input catalogue

We begin by identifying a large spectroscopic sample of galaxies drawn from the SDSS Data Release 7 (DR7; Abazajian et al. 2009). We require that all galaxies have secure spectroscopic redshifts (zConf > 0.7), redshifts of $0.02 < z < 0.2$, photometric and spectroscopic classifications as galaxies, and extinction-corrected Petrosian apparent magnitudes of $14.0 \leqslant m_r \leqslant 17.77$.

We employ the photometric total stellar mass measurements of Mendel et al. (2013), which were estimated using the updated $g-$ and $r-$band photometry of Simard et al. (2011), along with new photometry in the $u-$ and $i-$bands. We note that the photometry of Simard et al. (2011) has been shown to provide a significant improvement over the standard SDSS pipeline, especially for galaxies in crowded systems such as close pairs (Patton et al. 2011). Following Patton et al. (2011), we take full advantage of this improved photometry by requiring that each galaxy's observed fibre $g - r$ colour be within 0.1 mag of its Simard et al. (2011) model-predicted fibre colours. This yields an input catalogue of ∼ 607 000 galaxies for which secure redshifts and stellar masses are available.

2.2 Pair and environmental classifications

For every galaxy in this catalogue, we identify the closest neighbour, and characterize the environment with several additional measurements. We define the closest neighbour to be the galaxy with the smallest projected physical separation (hereafter r_p) which has a rest-frame relative velocity (hereafter Δv) of < 1000 km s^{-1} and is within a factor of 10 of the galaxy's stellar mass. We also record the projected separation of the second closest neighbour (hereafter r_2) and the total number of neighbours within 2 Mpc (hereafter N_2).

2.3 Star formation rate measurements

We now focus on galaxies which have secure SFR measurements, in order to examine how the presence of nearby companions (with or without SFR measurements) affects galactic star−forming properties. Our SFR measurements are drawn from the catalogue of Brinchmann et al. (2004), which has been updated to include DR7. Following Scudder et al. (2012), we restrict our analysis to fibre SFRs only. We require each galaxy to be classified as star-forming using the criteria of Kauffmann et al. (2003), and we require a signal−to−noise ratio of at least one in each of the emission lines used for this classification. These criteria yield a sample of ∼ 211 000 star-forming galaxies. No SFR requirements are imposed on neighbouring galaxies; therefore, our sample will include star forming members of both 'wet' and 'mixed' galaxy pairs.

2.4 Control sample

We wish to determine the influence (if any) that nearby companions have on the star−forming properties of galaxies. A common approach is to compare with a control sample of galaxies which have similar selection criteria but no close companions (e.g., Ellison et al. 2008; Patton et al. 2011; Scudder et al. 2012). However, this approach is robust only for relatively close companions; extending this approach to wider separations yields a control sample whose galaxies are substantially more isolated than the paired galaxies they are being compared with.

One method of dealing with this issue is to match paired and control galaxies on local density (Ellison et al. 2010; Scudder et al. 2012). However, as local density probes a substantially larger scale than the pairs, this matching cannot account for important differences in the smaller scale environment, as exemplified by compact groups embedded in loose groups (Mendel et al. 2011). Another approach is to require that both pairs and control galaxies be isolated on larger scales (Barton et al. 2007). However, as most galaxies reside in groups or clusters, this may remove the majority of the sample under consideration. Instead, we introduce a new methodology which addresses this issue by matching the control sample in both local density and isolation. A brief description of this method is provided here, with additional details and validation deferred to a subsequent paper (Patton et al. in preparation).

For each galaxy, we identify a control sample which is matched in stellar mass, redshift, local density, and isolation. We begin by requiring each control galaxy to be within 0.01 in redshift and 0.1 dex in stellar mass. We then use N_2 as a proxy for local density (which is reasonable given the match in redshift and stellar mass), and require that the N_2 of a galaxy and its controls agree within 10 percent. Finally, to match in isolation, we require the r_p of the control galaxy's closest companion to be within 10 per cent of the distance to the galaxy's second closest companion (r_2). Control galaxies are chosen with replacement, yielding an average of 34 controls for each galaxy. We determine weighted mean properties of each galaxy's control sample, assigning higher statistical weights to the control galaxies which provide the best simultaneous matches in z, mass, N_2 and r_2. This approach yields excellent agreement between galaxies and their controls in the four properties that are being matched. The same statistical weights are then also used to compute the mean SFR of the controls for each galaxy.

3 ENHANCED STAR FORMATION IN SDSS PAIRS

Armed with the SFRs of galaxies and their statistical control samples, we now proceed with a direct comparison between the two, as a function of pair separation. First, following Scudder et al. (2012), we restrict our analysis to pairs with $\Delta v < 300$ km s^{-1}, thereby focusing on the pairs which are most likely to be undergoing interactions. Next, we must account for the under-selection of close angular pairs (< 55 arcsec) in SDSS due to fibre collisions. Ellison et al. (2008) dealt with this effect by randomly culling 67.5 per cent of pairs with separations > 55 arcsec, using the results of the Patton & Atfield (2008) census of SDSS pairs. We instead apply a statistical weight w_θ (as defined in Patton et al. 2002) of 3.08 to each galaxy in close angular pairs ($w_\theta = 1/(1 - 0.675)$), thereby avoiding a cull of the wide pairs crucial to this analysis.

In the lower panel of Fig. 1, we plot the mean SFR of paired and control galaxies as a function of r_p. In the upper panel of the same figure, we plot the ratio of pairs versus control SFRs, which we interpret as the enhancement of SFR due to interactions (a ratio of one means no enhancement). At small separations, paired galaxies are found to have substantially higher SFRs than controls (up to a factor of 3), with very high statistical significance. Pair SFRs exhibit moderate enhancements of ∼ 20 per cent over the range $50 < r_p < 120$ kpc, and then decline to match their controls by

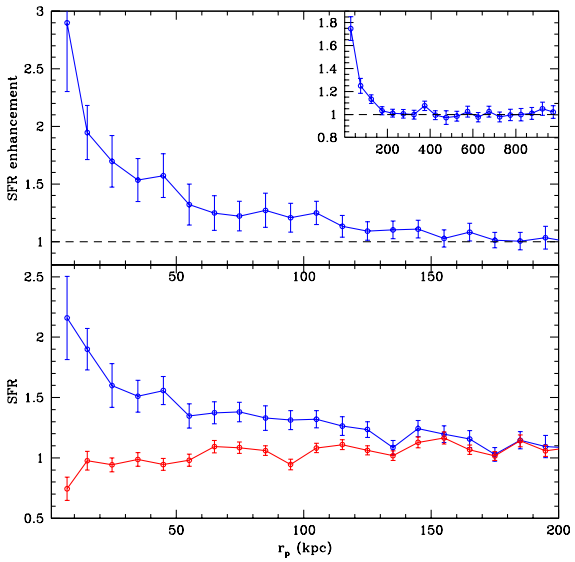

Figure 1. Lower panel: the mean SFR of SDSS paired galaxies (blue symbols) and their associated control galaxies (red symbols) is plotted versus projection separation (r_p). Upper panel: mean SFR enhancement (ratio of pair SFR to control SFR) is plotted versus r_p, with the dashed horizontal line denoting zero enhancement. The inset plot extends this out to 1000 kpc, using larger r_p bins. All error bars show the standard error in the mean.

Figure 2. This SDSS *gri* image shows a wide galaxy pair (r_p = 91 kpc) with an obvious tidal tail linking the member galaxies. Tidal features are also seen on the opposite side of each galaxy. The galaxy on the right (SDSS objID=587736619324735891) has an SFR of 7.8 $M_\odot$ yr^{-1}, which is 5.6 times higher than its controls. The companion galaxy is not in our star-forming sample, since it has a composite spectrum (star formation + AGN).

$r_p \sim 150$ kpc. Fig. 2 shows a striking example of enhanced star formation in a relatively wide pair (91 kpc) with a clear tidal tail linking the member galaxies. Above 150 kpc, there is no evidence of net enhancement (or suppression) in the pair SFR (this is true out to at least 1000 kpc, as shown in the inset panel of Fig. 1).

Over the range $r_p < 80$ kpc, these results are broadly consistent with the findings of Scudder et al. (2012), despite some differences in data (e.g., stellar masses, S/N requirements), pair selection, and environmental matching. At larger separations, our results indicate that we have achieved our goal of measuring SFR enhancements out to sufficiently wide separations that the enhancements reach zero. Since our paired galaxies have controls which are closely matched in galaxy properties (stellar mass and z) and environment (local density and isolation), we conclude that galaxy−galaxy interactions appear to be able to boost the mean SFR out to $r_p \sim 150$ kpc, but not further. If true, this implies that enhanced star formation extends out to larger separations than has previously been appreciated, and that studies of strongly interacting galaxies may miss a sizeable population of galaxies which exhibit enhanced star formation due to recent close encounters. To examine if this interpretation is physically plausible, we now turn to simulations.

4 *N*–BODY/SMOOTHED PARTICLE HYDRODYNAMICS (SPH) SIMULATIONS

4.1 Overview of the Simulations

We investigate the possibility that mergers are responsible for the observed SFR enhancement using a controlled suite of numerical simulations. The numerical methods employed here are similar to those described in detail in Torrey et al. (2012). Specifically, our simulation suite has been run using the N-Body/SPH simulation code GADGET (Springel 2005) which – in addition to including gravity and hydrodynamics – accounts for radiative cooling of gas (Katz, Weinberg, & Hernquist 1996), a density−driven SFR prescription with associated feedback (Springel & Hernquist 2003), and gas recycling from aging stellar populations (Torrey et al. 2012).

Our goal is to construct a set of galaxy merger simulations, where we can compare the evolving SFRs in isolated galaxies to the SFRs in merging systems, as a function of galactic separation r. To achieve this, we construct two isolated galaxies of initial stellar mass $M_1 = 5.7 \times 10^9 M_\odot$ and $M_2 = 1.4 \times 10^{10} M_\odot$. These masses, and the resulting stellar mass ratio of $\sim 2.5 : 1$, were chosen to match the median mass and mass ratio of our SDSS pairs sample. Each isolated galaxy contains a dark matter halo, a stellar and gaseous disc (20 per cent initial gas fraction), and a stellar bulge (which contains 20 per cent of the stellar mass). We ensure that our galaxies are stable against bar formation or other instabilities when evolved in isolation, and then set them on merging trajectories as described in the following subsection. Since our isolated galaxies are stable against bar formation or any rapid changes in their SFR, any major changes seen in the SFR for the merging galaxies can be confidently attributed to the merger interaction.

4.2 A suite of 75 merger simulations

For our merger suite, we adopt a set of five eccentricities (0.85, 0.9, 0.95, 1 and 1.05) and five impact parameters (2, 4, 8, 12 and 16 kpc) which are consistent with orbital element distribution functions derived from cosmological simulations (Wetzel 2011). While many previous merger studies have limited their scope to studying zero energy orbits with fixed impact parameters, the 25 combinations of eccentricity and impact parameter used in our merger suite yields substantial differences in the resulting apocentre separations ($r_{\rm apo}$). This is critical for this Letter, where we are interested in assessing the feasibility of driving SFR enhancements at relatively large galactic separations (> 100 kpc) via galaxy−galaxy interactions. Since there are no known correlations between the orientation of each galaxies' angular momentum vector relative to the

plane of the merger (e.g. Khochfar & Burkert 2006), we select three representative merger disc orientations (the e, f and k orientations from Robertson et al. 2006), yielding a suite of 75 merger simulations. We emphasize that this merger suite is not intended to be complete, as we are still failing to sample a large portion of available merger parameter space (e.g., variations in galaxy morphology, mass, mass ratio, gas fraction, etc.). Moreover, these simulated pairs are pure binary systems, without the cosmological context of additional galaxies spanning a range of environments. However, by including a range of orbital parameters as we have done here, we gain specific insight about interaction-driven starburst activity at large galactic separations which has not been previously extensively studied.

We track the total and central (within 1 kpc) SFR of each simulated galaxy as a function of time. In order to facilitate comparison with our SDSS sample, we translate the simulated SFRs into SFR enhancements by normalizing by the SFR of the galaxy when evolved in isolation. In Fig. 3, we show how pair separation and total SFR enhancement depend on the time relative to first pericentre passage ($t_{\rm peri}$) for a representative subset of orbital configurations in this merger suite. The resulting $r_{\rm apo}$ varies from ~55 to 220 kpc, with the largest $r_{\rm apo}$ corresponding to the highest eccentricity and largest impact parameter (and vice versa).

For each of the orbits shown in Fig. 3, a strong burst of star formation begins shortly after the first close passage, with a maximum SFR enhancement of a factor of 1.3–2.2. This enhancement persists for about 1.5 Gyr for all orbits in which the galaxies remain apart from one another during this timeframe. In every case, a second and stronger burst of star formation begins shortly before coalescence. For orbits with relatively high eccentricities and impact parameters, there is enough time for the first episode of enhanced star formation to subside, followed by a period of suppressed star formation (quenching). This intriguing result would not have been seen if, like many other studies, we had restricted our orbits to low eccentricities and small impact parameters.

4.3 SFR enhancements as a function of r_p

In order to compare these results with our SDSS measurements of SFR enhancements (Fig. 1), we observe each of these orbits from a large number of random orientations, and at random times during the orbits, computing r_p and Δv in each case. While the simulated orbits begin at a initial separation of 165 kpc (corresponding to the virial radius of the more massive galaxy), we extrapolate each orbit backward in time to an initial separation of 10 Mpc, to ensure that we follow each orbit for effectively all the time that the pair has $r_p < 200$ kpc. We then compute the average SFR enhancement over all 75 orbital configurations, treating each 10 Myr timestep equally, which accounts for the fact that some orbits take longer to coalesce than others. We exclude all data points for which $\Delta v > 300$ km s^{-1}, as was done with our SDSS pairs. The results are shown in Fig. 4 (the corresponding error bars are vanishingly small, since we average over so many viewing angles).

Within the simulations, we see strong SFR enhancements at small separations ($r_p < 10$ kpc) which are driven by coalescing systems. The simulations yield moderate enhancements at a wide range of separations (roughly 20-100 kpc), with smaller enhancements extending out to ~ 150 kpc. As seen in Fig. 4, the total and central SFR enhancements in the simulations roughly bracket the SDSS enhancements, with a similar dependence on r_p. These simulations suggest that the SFR enhancements seen in widely separated SDSS pairs are the result of star formation triggered by earlier close

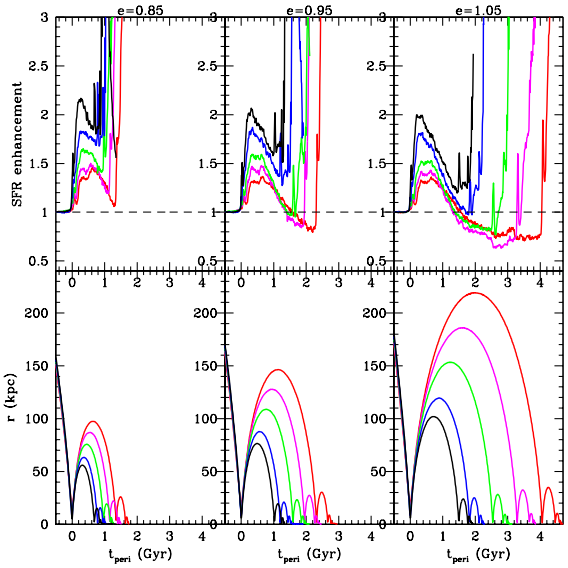

Figure 3. A subset of our suite of simulated orbits is shown. The lower panels depict 3D pair separation (r) versus time since first pericentre ($t_{\rm peri}$). The upper panels show how the total SFR enhancement varies with $t_{\rm peri}$, with the horizontal dashed lines denoting zero enhancement. The left–hand, middle and right–hand columns correspond to eccentricities of 0.85, 0.95, and 1.05 respectively. The colour scheme depicts impact parameters of 2 kpc (black), 4 kpc (blue), 8 kpc (green), 12 kpc (magenta), and 16 kpc (red). For clarity, we plot only the f disc orientation, which generally has SFR enhancements between the e and k disc orientations.

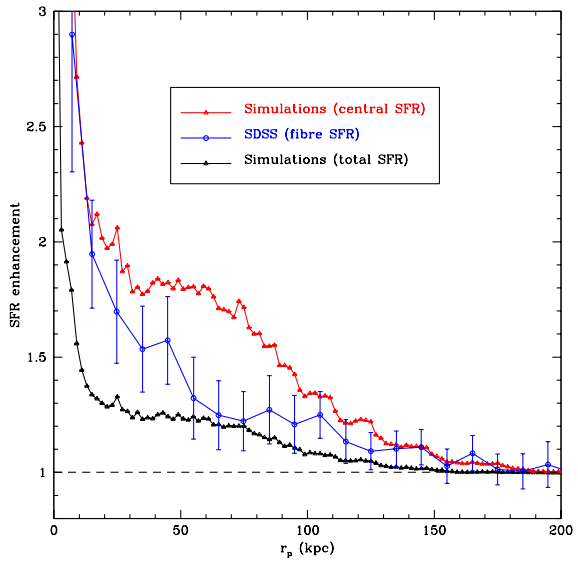

Figure 4. Mean SFR enhancement is plotted versus projected separation (r_p) for both the simulations (black and red symbols) and the observations (blue; from Fig. 1). The horizontal dashed line denotes zero SFR enhancement. The SDSS SFRs are measured using fibres with a median projected radius of 2.5 kpc, whereas the central SFRs for the simulations are computed within a 3D radius of 1 kpc.

passages. In the simulations, it typically takes ~ 1 Gyr for galaxies to reach $r_p \sim 150$ kpc after their first close passage, travelling at a time-averaged transverse speed of ~ 150 km s^{-1}. This is consistent with the relatively long time-scale of enhanced star formation seen in Fig. 3.

5 DISCUSSION

We have found clear evidence of enhanced star formation in pairs with separations as large as 150 kpc, and have demonstrated that such enhancements can be produced in simulations with realistic orbits. The rise in enhancements towards the smallest scales and the absence of any net enhancement on larger scales is consistent with star formation triggered by galaxy−galaxy interactions.

Although it has been appreciated that mergers can drive starburst activity following close passages (e.g., Barnes & Hernquist 1996), much of the focus has been on very close separations associated with final coalescence. Here, we have used numerical simulations to show that this same physical picture can apply to SFR enhancements that occur at large galactic separations following first pericentre passage. Specifically, since there is a time delay between close passages and peak starburst activity of the order of an orbital or dynamical time, it is possible for SFR enhancements to appear prominently at large galactic separations as the galaxies separate after first pericentre passage.

While a detailed census of interacting/merging pairs is beyond the scope of this Letter, we can estimate the fraction of star forming galaxies which are found in these wider pairs. Following Patton et al. (2000), we weight the observed pair fraction by the reciprocal of the overall spectroscopic completeness of the survey (88 per cent according to Patton & Atfield 2008), and also weight close angular pairs by an additional factor of 3.08 (see Section 3), and find that 12.3 per cent of galaxies are in $r_p < 150$ kpc pairs, versus 1.8 per cent in $r_p < 30$ kpc pairs. Moreover, by applying this methodology to the data in the lower panel of Fig. 1, we estimate that of the enhanced star formation occurring in pairs with $r_p < 150$ kpc, 66 per cent occurs at $r_p > 30$ kpc. This implies that interaction-induced star formation is much more prevalent than has been appreciated to date.

We caution that our SDSS sample is not complete for the 1:10 stellar mass ratio pairs considered in this study, and we have not attempted to correct for this in our rough census. We note also that our SDSS paired galaxies (and their controls) were required to have secure SFR measurements; as a result, our sample is restricted primarily to 'blue cloud' galaxies which lie on the star-forming sequence (Salim et al. 2007). Finally, we cannot rule out enhancements in individual pairs at even wider separations (including flybys); however, any such enhancements appear, to first order, to be cancelled out by the suppression of star formation in other pairs.

We caution also that we have used a rather simple suite of merger simulations to demonstrate consistency between the observations and simulations. While this has the advantage of clarity, future studies will be able to improve on this by using a merger suite that more closely matches the properties of paired galaxies found in SDSS. This can be achieved by using a substantially larger merger suite, allowing for coverage or exploration of a more complete portion of the merger parameter space. Or, it may be possible to take advantage of continued advancements in computational resources and numerical methods to measure SFR enhancements directly from cosmological hydrodynamical simulations. Recent studies have shown improvements in the ability of galaxies to form and maintain gas–rich discs in cosmological simulations (Vogelsberger et al. 2012; Torrey et al. 2012) which may allow for direct measures of the SFR enhancement for paired galaxies using analogous methods to those applied in our SDSS analysis.

6 CONCLUSIONS

We have used a well-defined sample of $\sim 211\,000$ star-forming galaxies to measure SFR enhancements as a function of pair separation. Our novel method of characterizing the local density and isolation of paired galaxies yields the first secure measurements of enhancements at wide separations. We find that SFR enhancements are detectable out to $r_p \sim 150$ kpc, with no net enhancement (or suppression) seen at larger separations. As with earlier work, we find the strongest enhancements at the smallest pair separations. We have compared these results with the predictions from a suite of *N*–body/SPH simulations of merging galaxies, and find broad agreement. In particular, the enhancements seen out to ~ 150 kpc are a natural outcome of mergers in which the eccentricities and impact parameters are sufficiently high to lead to the required separations before the interaction–induced SFR enhancements subside.

REFERENCES

Abazajian K. N., et al., 2009, ApJS, 182, 543
Barnes J. E., Hernquist L., 1996, ApJ, 471, 115
Barton E. J., Geller M. J., Kenyon S. J., 2000, ApJ, 530, 660
Barton E. J., Arnold J. A., Zentner A. R., Bullock J. S., Wechsler R. H., 2007, ApJ, 671, 1538
Brinchmann J., Charlot S., White S. D. M., Tremonti C., Kauffmann G., Heckman T., Brinkmann J., 2004, MNRAS, 351, 1151
Cox T. J., Jonsson P., Somerville R. S., Primack J. R., Dekel A., 2008, MNRAS, 384, 386
Di Matteo P., Combes F., Melchior A.-L., Semelin B., 2007, A&A, 468, 61
Ellison S. L., Patton D. R., Simard L., McConnachie A. W., 2008, AJ, 135, 1877
Ellison S. L., Patton D. R., Simard L., McConnachie A. W., Baldry I. K., Mendel J. T., 2010, MNRAS, 407, 1514
Ellison S. L., Patton D. R., Mendel J. T., Scudder J. M., 2011, MNRAS, 418, 2043
Ellison S. L., Mendel J. T., Scudder J. M., Patton D. R., Palmer M. J. D., 2013, MNRAS, 430, 3128
Katz N., Weinberg D. H., Hernquist L., 1996, ApJS, 105, 19
Kauffmann G., et al., 2003, MNRAS, 346, 1055
Khochfar S., Burkert A., 2006, A&A, 445, 403
Lambas D. G., Tissera P. B., Alonso M. S., Coldwell G., 2003, MNRAS, 346, 1189
Mendel J. T., Ellison S. L., Simard L., Patton D. R., McConnachie A. W., 2011, MNRAS, 418, 1409
Mendel, J. T. et al. 2013, ApJS, submitted
Mihos J. C., Hernquist L., 1996, ApJ, 464, 641
Montuori M., Di Matteo P., Lehnert M. D., Combes F., Semelin B., 2010, A&A, 518, A56
Park C., Choi Y.-Y., Vogeley M. S., Gott J. R., III, Blanton M. R., SDSS Collaboration, 2007, ApJ, 658, 898
Patton D. R., Atfield J. E., 2008, ApJ, 685, 235
Patton D. R., Carlberg R. G., Marzke R. O., Pritchet C. J., da Costa L. N., Pellegrini P. S., 2000, ApJ, 536, 153
Patton D. R., et al., 2002, ApJ, 565, 208
Patton D. R., Ellison S. L., Simard L., McConnachie A. W., Mendel J. T., 2011, MNRAS, 412, 591
Robaina A. R., et al., 2009, ApJ, 704, 324
Robaina A. R., Bell E. F., 2012, MNRAS, 427, 901

Robertson B., Cox T. J., Hernquist L., Franx M., Hopkins P. F., Martini P., Springel V., 2006, ApJ, 641, 21
Salim S., et al., 2007, ApJS, 173, 267
Scudder J. M., Ellison S. L., Torrey P., Patton D. R., Mendel J. T., 2012, MNRAS, 426, 549
Simard L., Mendel J. T., Patton D. R., Ellison S. L., McConnachie A. W., 2011, ApJS, 196, 11
Sol Alonso M., Lambas D. G., Tissera P., Coldwell G., 2006, MNRAS, 367, 1029
Springel V., 2005, MNRAS, 364, 1105
Springel V., Hernquist L., 2003, MNRAS, 339, 289
Torrey P., Cox T. J., Kewley L., Hernquist L., 2012a, ApJ, 746, 108
Torrey P., Vogelsberger M., Sijacki D., Springel V., Hernquist L., 2012b, MNRAS, 427, 2224
Vogelsberger M., Sijacki D., Kereš D., Springel V., Hernquist L., 2012, MNRAS, 425, 3024
Wetzel A. R., 2011, MNRAS, 412, 49
Woods D. F., Geller M. J., Kurtz M. J., Westra E., Fabricant D. G., Dell'Antonio I., 2010, AJ, 139, 1857